**ASTROPHYSICS**

**(stellar atmospheres, interacting binary systems, variable stars)**

https://doi.org/10.18524/1810-4215.2025.38.343166

# PERIODIC VARIATIONS IN THE OPTICAL SPECTRUM OF THE POST-AGB OBJECT LN HYA

S. E. Achkassova[1], Sh. T. Nurmakhametova[1], A. S. Miroshnichenko[1,2,3], N. L. Vaidman[2,1], S. A. Khokhlov[2,1], D. T. Agishev[1], S. Danford[3]

[1] Al-Farabi Kazakh National University, Al-Farabi Ave, 71, 050040, Almaty, Kazakhstan, *snezhanachkasova29@gmail.com*; *shahidanurmahametova@gmail.com*; *agishev.pluto@gmail.com*

[2] Fesenkov Astrophysical Institute, Observatory, 23, 050020 Almaty, Kazakhstan, *nva1dmann@gmail.com*; *skhokh88@gmail.com*

[3] Department of Physics and Astronomy, University of North Carolina at Greensboro, Greensboro, NC 27402-6170, USA, *a_mirosh@uncg.edu*; *danford@uncg.edu*

ABSTRACT. LN Hya (BS 4912; HD 112374) has long been regarded as a post-AGB F-type supergiant, located at a high Galactic latitude ($b = +36\overset{\circ}{.}3$). Earlier studies relied on limited spectroscopic and photometric material. We present a new data set comprising 73 medium-resolution ($R \approx 12{,}000$) optical spectra obtained at the 0.81-meter telescope of the Three College Observatory (North Carolina, USA) in 2021—2025. We found regular variations in the radial velocities (RV) of absorption lines with a period of $148.63 \pm 0.09$ days. Our observations cover 10 most recent variability cycles and suggest that LN Hya is a binary system with an eccentric orbit ($e = 0.19 \pm 0.02$). In this paper, we describe the data reduction and analysis process as well as some spectral features of the system. Future plans for a deeper study of LN Hya that include analyzing existing photometric data and correlating them with the spectral variability are outlined.

**Keywords**: post-AGB stars; binary systems; spectroscopic orbits; radial velocities; stellar variability.

АНОТАЦІЯ. LN Hya (BS 4912; HD 112374) довгий час вважався надгігантом типу F після AGB, розташованим на високій галактичній широті ($b = +36\overset{\circ}{.}3$). Раніше дослідження спиралися на обмежений спектроскопічний та фотометричний матеріал. Ми представляємо новий набір даних, що містить 73 оптичні спектри середньої роздільної здатності ($R \approx 12\ 000$), отримані на телескопі діаметром 0,81 м Обсерваторії Трьох Коледжів (Північна Кароліна, США) у 2021—2025 рр. Ми виявили регулярні варіації радіальних швидкостей (RV) ліній поглинання з періодом 148,63 ± 0,09 днів. Наші спостереження охоплюють 10 останніх циклів змінності та свідчать, що LN Hya є подвійною системою з ексцентричною орбітою ($e = 0{,}19 \pm 0{,}02$). У цій роботі ми описуємо процес редукції та аналізу даних, а також деякі спектральні особливості системи. Окреслено плани подальшого детальнішого дослідження LN Hya, що включають аналіз наявних фотометричних даних і їх кореляцію зі спектральною варіабельністю.

**Ключові слова**: зорі після AGB; подвійні системи; спектроскопічні орбіти; радіальні швидкості; зоряна змінність.

## 1. Introduction

Post-AGB stars are evolved low- and intermediate-mass objects (initial masses 0.8–8 $M_\odot$). They represent a short-lived ($\sim 10^3$–$10^4$ yr) transitional stage between the asymptotic giant branch (AGB) and the planetary nebula. During this phase, the star loses most of its extended outer envelope, which forms a circumstellar shell rich in gas and dust. As the envelope disperses, the star evolves toward higher effective temperatures on the Hertzsprung–Russell diagram. It contracts and heats up while still retaining the luminosity characteristic of a cool supergiant. The effective temperature ($T_{\rm eff}$) increases from ∼5,000 K to as high as 30,000–200,000 K for the hottest remnants (Miller Bertolami 2016). Meanwhile, the core temperature remains on the order of 10–100 MK. This evolutionary stage typically ends with the star becoming the central star of a planetary nebula and, ultimately, a white dwarf (Van Winckel 2003; Herwig 2005).

One of the brightest stars in its class is LN Hya (BS 4912, HD 112374). It is located at a high Galactic

latitude of $b = +36.4°$ and exhibits a noticeable metal deficiency, which confidently places it among the old stellar population, likely belonging to the thick disk or Galactic halo. Its bolometric luminosity, estimated as $\log(L/L_\odot) = 4.0$, along with $T_{\rm eff} \simeq 6000$ K, places LN Hya close to the post-AGB evolutionary track with a core mass $M_{\rm core} \approx 0.6\,M_\odot$ in the models of Miller Bertolami (2016), consistent with other similar post-AGB objects (e.g., Klochkova, Panchuk 2012).

The optical spectrum of LN Hya corresponds to an F-type luminous supergiant (F3 Ia). It shows typical characteristics of low-mass, post-AGB "high-latitude supergiants". One notable feature is the H$\alpha$ line profile, which usually displays emission components superimposed on a broad absorption. Among post-AGB stars, the H$\alpha$ line is commonly observed to exhibit a double-peaked emission profile, a hallmark of a rotating circumstellar structure. In some systems, the emission arises in material gravitationally bound to the primary star and situated outside its orbit. It likely forms in a circumbinary disk and varies with the orbital phase (e.g., Nurmakhametova et al. 2025). In other cases, the H$\alpha$ profile appears as a deep absorption core partially filled in by emission wings. Such profiles are commonly interpreted as evidence of a long-lived reservoir of the circumstellar gas distributed in a rotating disk or an extended envelope (e.g., Klochkova, Panchuk 2012).

Post-AGB binaries with long-lived circumbinary dusty disks form a well-studied class: their SEDs show stable near-IR excesses from compact Keplerian disks, now resolved interferometrically and modeled as dust-sublimation–truncated rims (De Ruyter et al. 2006; Hillen et al. 2017; Kluska et al. 2019). Their orbital periods span $\sim 10^2$–$10^3$ days and frequently retain significant eccentricities, likely sustained or re-excited by disk–binary interactions (Dermine et al. 2013; Oomen et al. 2018). In this context, LN Hya's RV period, H$\alpha$ phenomenology, and other spectral properties place it among the disk-bearing post-AGB binaries, where binarity, mass loss, and disk dynamics are coupled.

Luck et al. (1983) found the following fundamental parameters of LN Hya: $T_{\rm eff} \simeq 6000$K, a surface gravity of $\log g = 0.4$ - $0.8$ and a significantly reduced metallicity of [Fe/H] = –1.2, accompanied by a nitrogen overabundance of [N/Fe] = +0.5.

Despite previous observations, LN Hya remains an object of a considerable interest due to its atmospheric instability, variable emission characteristics, and unusual chemical abundance patterns, characterized by a significant depletion of refractory elements (e.g., Fe, Ca, Ti) and an enhancement of nitrogen ([Fe/H] ≈ –1.2, [N/Fe] ≈ +0.5). Such selective abundance anomalies are typical of post-AGB binaries with circumbinary disks, where refractory elements condense into dust grains while volatile species are re-accreted onto the stellar atmosphere. Previous investigations of LN Hya were hampered by the scarcity of high-resolution, homogeneous spectroscopic material and the absence of a long-term RV monitoring.

Revealing the binary nature of LN Hya is crucial for understanding the origin of its circumstellar matter, the mass-loss mechanisms, and the role of binarity in the post-AGB evolution. In this context, our new multi-year spectroscopic campaign provides the first opportunity to derive a coherent orbital solution and directly test the binary hypothesis.

The primary aim of this work is to perform a high-resolution spectroscopic and photometric analysis of LN Hya, focusing on the temporal behavior of key spectral lines, particularly H$\alpha$, as well as RV variations that may reflect atmospheric pulsations or dynamical instabilities. In addition, we aim to derive the orbital parameters of the system by analyzing long-term RV data, with the goal of verifying the possible binary nature of LN Hya and detecting a potential secondary component. Photometric observations will also be used to study brightness variations and light curve morphology, offering further insights into the physical processes governing the evolution and variability of this post-AGB object.

## 2. Observations

Spectroscopic monitoring was carried out with the 0.81 m telescope at the Three College Observatory using the échelle spectrograph eShel (Shelyak Instruments[1]) between 19 May 2021 and 2 June 2025. In total, 73 spectra were obtained. Because the target remains low at the site (latitude $+35°56'$), typical total integrations were 1-2 hours, composed of individual 25–40–minute exposures.

The data reduction did not include overscan removal or dark-frame subtraction. Dark frames were used only to identify and map detector pixels that show abnormal responses, producing artificial narrow emission-like features. These "bad" pixels were recorded into a mask and corrected during the initial processing using the fixpix task in the ccdproc package, which proved to be more efficient and stable than traditional dark subtraction. The remaining steps of the procedure comprised scattered-light suppression, order tracing and optimal extraction, wavelength calibration with ThAr-lamp spectra, heliocentric correction, and continuum normalization with masking of strong spectral features. Flat-field frames were not applied because the detector's pixel-to-pixel sensitivity variations are $\leq 1.5\%$, and the flat-field lamp does not illuminate the full extracted spectral range. The typical accuracy of the wavelength solution is on the order of a few $10^2\,{\rm m\,s^{-1}}$ ($\approx 300\,{\rm m\,s^{-1}}$).

[1] https://shelyak.com

## 3. Methods

RVs were measured by cross-correlation in the spectral window $\lambda$ = 5046–5163 Å, which is rich in narrow metallic lines and minimally affected by emission or telluric contamination. Before computing the CCF, residual outliers were removed, the continuum was normalized, and problematic segments were masked. The cross-correlation peak was fitted with a Gaussian; the centroid yields the RV, while the width and contrast provide the internal uncertainty. To account for excess scatter beyond the formal errors, we introduced an additive jitter term, $\sigma_j$, as a free parameter in the Markov-Chain Monte Carlo (MCMC) analysis. This approach provides a robust, fully Bayesian estimation of the orbital parameters, properly propagating non-Gaussian uncertainties and correlations between parameters such as $P$, $e$, and $K_1$. This method yields posterior probability distributions rather than single best-fit values, allowing realistic credible intervals for each element of the orbit. This term, typically 0.4–0.8 km s$^{-1}$, absorbs additional astrophysical or instrumental variability. A systematic error floor of the same order was also adopted to reflect instrumental stability. The RV zero point was monitored via stable spectral regions and inter-night consistency checks.

As a reference template for cross-correlation, we used our spectrum of LN Hya obtained on 2021/05/19 (see Fig. 1), which has a S/N ratio of $\sim$ 200 in the continuum of the chosen region. The orbital RV for the template spectrum was determined by cross-correlating the mentioned spectral region with that of a constant RV star $\alpha$ Persei (RV$_{\rm hel} = -2.1$ km s$^{-1}$) obtained with the same equipment. This way the RV scale was translated into the heliocentric frame (see Fig. 2).

RVs were analysed with a reproducible analysis pipeline implemented in Python. First, we determined the period from the RV time series using the Lomb–Scargle algorithm, which is appropriate for uneven sampling and highlights the dominant periodicity. Next, we modelled the RV curve with a single-lined Keplerian profile and inferred the orbital elements by Bayesian Markov-chain Monte Carlo sampling using the affine-invariant ensemble sampler implemented in the `emcee` package (Foreman-Mackey et al., 2013).

We used weakly informative priors, initialized chains near the periodogram solution, discarded burn-in, and checked convergence with standard diagnostics. Final values for the period, systemic velocity, semi-amplitude, eccentricity, and argument of periastron are reported as posterior medians with 16th–84th percentile credible intervals. The workflow follows our previously published RV+MCMC analyses and is implemented in Python. This method was also employed in Vaidman et al. (2025a) and in Nurmakhametova et al. (2025); see also Vaidman et al. (2025b) for methodological details.

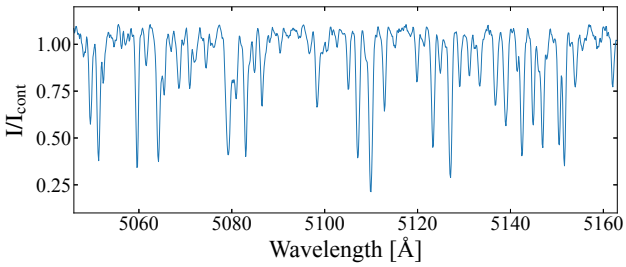


Figure 1: Part of the TCO spectrum of LN Hya in the wavelength range 5046–5163 Å obtained on 2021/05/19 and used as a template for cross-correlation.

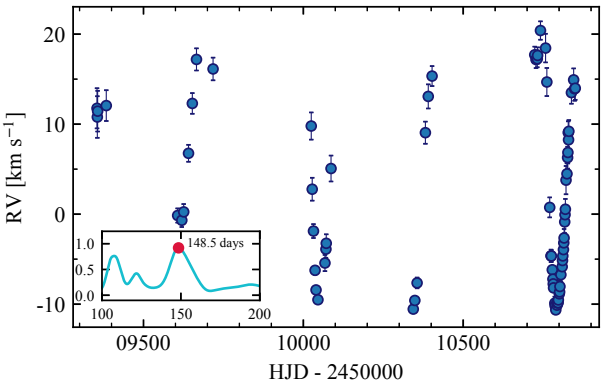


Figure 2: RV measurements in the heliocentric frame as a function of HJD. The inset shows the periodogram, indicating a detected period of 148.5 days.

## 4. Results

The LS periodogram (inset in Fig. 2) shows a single dominant peak at a period of 148.5 days with a very low false-alarm probability; weaker aliases are negligible. Folding the RVs on this period produces a phase-coherent curve with minimal scatter, consistent with the modulation seen in the long-term photometry. This establishes the characteristic timescale of the system and underpins the orbital solution reported below. The phase-folded RV curve (Fig. 3) for the first time demonstrates that LN Hya is a spectroscopic binary. The smooth line approximating the data points is the best-fitting single-lined Keplerian (SB1) model, computed from the MCMC posterior-median orbital elements listed in Table 1.

The phase–coherent RV curve establishes a well-constrained single–lined spectroscopic orbit for LN Hya (Table 1). The solution indicates a moderate eccentricity with a well–constrained argument of periastron, a stable systemic velocity across all seasons, and a precisely measured semi–amplitude of the visible

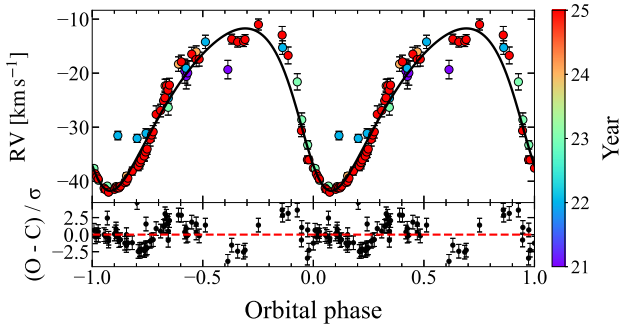


Figure 3: Radial velocity of LN Hya in the 10 latest orbital cycles ($\sim$ 1,500 days). RVs were measured in the TCO spectra by cross-correlation in a spectral range $\lambda$ = 5046–5163 Å. The colour scale indicates the year of observation.

Table 1: Orbital parameters of LN Hya.

| No. | Parameter | Value |
|---|---|---|
| 1 | $P$ (days) | $148.63 \pm 0.09$ |
| 2 | $T_0$ (HJD) | $2459291.31 \pm 1.83$ |
| 3 | $e$ | $0.19 \pm 0.02$ |
| 4 | $\omega$ (degrees) | $106.85 \pm 0.23$ |
| 5 | $\gamma$ (km s$^{-1}$) | $-24.29 \pm 0.34$ |
| 6 | $K_1$ (km s$^{-1}$) | $14.979 \pm 0.44$ |
| 7 | $f(m)$ ($M_\odot$) | $0.049 \pm 0.004$ |
| 8 | $N$ | 73 |

**Notes.** (1) Orbital period; (2) periastron epoch for the elliptical orbit and time of superior conjunction (at $\gamma$ RV) for the circular orbit; (3) eccentricity; (4) argument of the periastron; (5) systemic RV; (6) semi-amplitude of the RV variation of the visible component; (7) mass function; (8) number of spectra used in the orbit calculation.

component. This is the first self–consistent orbital solution for LN Hya solely based on a homogeneous RV data set. It determines the system's dynamical timescale and geometry for subsequent analysis.

## 5. Conclusions and Discussion

We present the first self-consistent spectroscopic orbit for LN Hya based solely on medium-resolution RVs. Our homogeneous data set and uniform Bayesian analysis yield a stable, repeatable single-lined solution; the derived elements are internally consistent and robust, fixing the system's dynamical timescale and geometry for the first time. The $\sim$148.5 days period inferred from the RV curve is too long for a classical pulsating Cepheid at the star's temperature and luminosity, favouring the orbital interpretation. The variability can plausibly arise from geometric and atmospheric effects within the binary (e.g., shallow eclipses and/or phase-dependent heating of the visible component).

A phase-coherent orbit enables: (i) mass-function limits on the unseen component and a pathway to dynamical masses once the inclination is constrained; (ii) predictive ephemeris to phase-tag follow-up spectroscopy and interferometry; (iii) separation of orbital signals from low-amplitude atmospheric pulsations; and (iv) phase-dependent modelling of circumbinary gas and dust within a self-consistent geometry.

**Future directions.** We will (i) extend and densify the RV monitoring to refine the orbital elements and mass function, especially near periastron; (ii) obtain higher-resolution spectra to search for weak features of the secondary and to improve line-profile modelling; and (iii) constrain the inclination via long-baseline (spectro-)interferometry and $v \sin i$ constraints to enable dynamical masses. These steps will deliver a more accurate orbital solution and provide deeper insights into the origin of the system.

*Funding.* This research was funded by the Science Committee of the Ministry of Science and Higher Education of the Republic of Kazakhstan (Grant No. AP23484898).

*Acknowledgements.* This research has made use of the SIMBAD database, operated at CDS, Strasbourg, France; SAO/NASA ADS, ASAS, and Gaia data products. This paper is based on observations obtained at the 0.81 m telescope of the Three College Observatory (North Carolina, USA). A.M. and S.D. acknowledge technical support from Dan Gray (Sidereal Technology Company), Joshua Haislip (University of North Carolina Chapel Hill), and Mike Shelton (University of North Carolina Greensboro), as well as funding from the UNCG College of Arts and Sciences and Department of Physics and Astronomy.

## References

Arkhipova V.P., Ikonnikova N.P., Noskova R.I., Komissarova G.V.: 2001, *Astron. Lett.*, **27**, 156–168.

Dermine T., Izzard R.G., Jorissen A., Van Winckel H.: 2013, *Astron. Astrophys.*, **551**, A50.

Foreman-Mackey D., Hogg D.W., Lang D., Goodman J.: 2013, *Publ. Astron. Soc. Pac.*, **125**, 306.

Henson G.D., Deskins W.R.: 2009, *ASP Conf. Ser.*, **412**, 229.

Herwig F.: 2005, *Annu. Rev. Astron. Astrophys.*, **43**, 435–479.

Hillen M., Van Winckel H., Menu J., Manick R., Debosscher J., Min M., de Wit W.-J., Verhoelst T., Kamath D., Waters L.B.F.M.: 2017, *Astron. Astrophys.*, **599**, A41.

Klochkova V.G., Panchuk V.E.: 2012, *Astron. Rep.*, **56**, 104–115.

Kluska J., Van Winckel H., Hillen M., et al.: 2019, *Astron. Astrophys.*, **631**, A108.

Luck R.E., Lambert D.L., Bond H.E.: 1983, *Publ. Astron. Soc. Pac.*, **95**, 413–421.

Miller Bertolami M.M.: 2016, *Astron. Astrophys.,* **588**, A25.

Nurmakhametova S.T., Vaidman N.L., Miroshnichenko A.S., Khokhlov A.A., Agishev A.T., Yermekbayev B.S., Danford S., Aarnio A.N.: 2025, *Galaxies,* **13**, 26.

Oomen G.-M., Van Winckel H., Pols O., Nelemans G., Escorza A., Manick R., Kamath D., Waelkens C.: 2018, *Astron. Astrophys.,* **620**, A85.

De Ruyter S., Van Winckel H., Maas T., Lloyd Evans T., Waters L.B.F.M., Dejonghe H.: 2006, *Astron. Astrophys.,* **448**, 641–653.

Vaidman N.L., Miroshnichenko A.S., Zharikov S.V., Khokhlov S.A., Agishev A.T., Yermekbayev B.S.: 2025a, *Galaxies,* **13**, 3, 47.

Vaidman N.L., Nurmakhametova S.T., Miroshnichenko A.S., Khokhlov S.A., Agishev A.T., Khokhlov A.A., Ashimov Y.K., Yermekbayev B.S.: 2025b, *Galaxies,* **13**, 5, 101.

Van Winckel H.: 2003, *Annu. Rev. Astron. Astrophys.,* **41**, 391–427.